Electronic Supplementary Information

Pnictogen Bonding in Imide Derivatives for Chiral Folding and Self-Assembly

Zhuoer Wang, Zhaozhen Cao, Aiyou Hao and Pengyao Xing*

School of Chemistry and Chemical Engineering, Shandong University, Jinan 250100, People's Republic of China.

1. Experimental

Materials

Reagents were obtained from commercial sources and used without further purification. 4-Bromo-1,8-naphthalic anhydride, 5-bromoisobenzofuran-1,3-dione, 1H,3H-benzo[de]isochromene-1,3-dione and 4,5,6,7-tetrafluoroisobenzofuran-1,3-dione were purchased from Energy Chemical Co. Ltd. (China). Aniline, 2-methoxyethan-1-amine and 2-aminophenol were purchased from Guoyao Chemical Reagent Co. Ltd., Shanghai. All amino acid methyl ester hydrochloride and alkamine were purchased from Bide pharm, China. Anhydrous ethanol, 1, 2 dichloroethane and methanol were purchased from Tianjin Fuyu Fine Chemical Co., Ltd. (China). All solvents were of reagent grade.

Quantum mechanical calculation of ECD spectrum

Absolute configuration of building units was extracted directly from X-ray crystal structures. Then, the B3LYP-D3/def2SVP basis set was utilized to calculate absorption/ECD spectra based on time-dependent density functional theory (TDDFT).

Instrumentation

^{1}H NMR spectra, ^{13}C NMR spectra were obtained by BRUKER AVANCE III HD 400. High-Resolution Mass Spectra (HR-MS) were performed on an Agilent Q-TOF 6510.

Circular dichroism (CD) was measured with an Applied Photophysics ChirascanV100 model. Single crystal was collected on Rigaku Oxford Diffraction XtaLAB Synergy diffractometer equipped with a HyPix-6000HE area detector (Japan), using a Mo Kα radiation (λ = 0.71073 Å) or Cu Kα radiation (λ = 1.54056 Å) from Photon Jet micro-focus X-ray source. Fourier transform infrared (FT-IR) measurements were performed on a Tensor II FT-IR spectrometer. X-ray diffraction (UK) with Cu Kα radiation (λ = 0.15406 nm, voltage 45 KV, current 200 mA, power 9 KW). The samples were casted onto cover glasses (18 mm × 18 mm) and dried to form thin films. Fluorescence lifetime and quantum yield (QY) were measured by Steady State-Transient-Fluorescence Spectrometer (Edinburgh FLS920). Fluorescence spectra was made on a RF 6000 Shimadzu fluorophotometer.

Synthesis

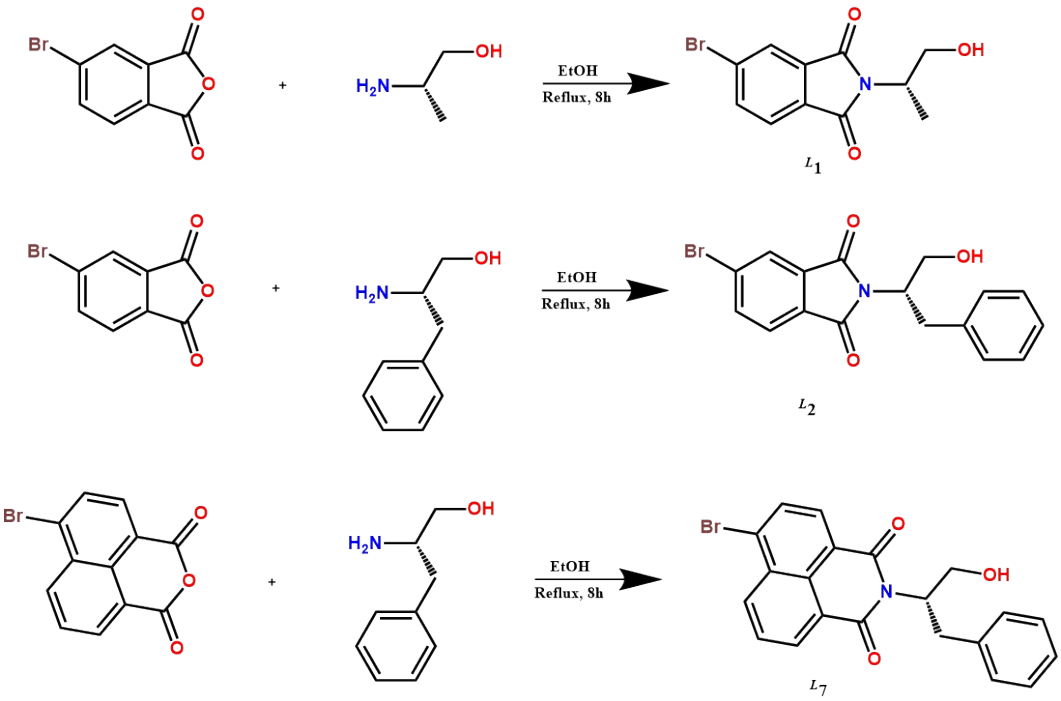

Synthetic route of imide derivatives.

Synthesis of compound ^{L}1: A mixture of 5-bromoisobenzofuran-1,3-dione (5 mmol, 1.13 g) and (S)-2-aminopropan-1-ol (5 mmol, 0.38 g) were dissolved in ethanol (25 mL). The above solution was refluxed at 80 °C for 8 h. After completion of reaction, further purified by silica gel column chromatography. ^{D}**1** was synthesized as the same procedures as ^{L}1.

Synthesis of compound ^{L}2: A mixture of 5-bromoisobenzofuran-1,3-dione (5 mmol, 1.13 g) and (S)-2-amino-3-phenylpropan-1-ol (5 mmol, 0.75 g) were dissolved in ethanol (25 mL). The above solution was refluxed at 80 °C for 8 h. After completion of reaction, further purified by silica gel column chromatography. ^{D}**2** was synthesized as the same procedures as ^{L}**2**.

Synthesis of compound ^{L}7: A mixture of 4-bromo-1,8-naphthalic anhydride (5 mmol, 1.37 g) and (S)-2-amino-3-phenylpropan-1-ol (5 mmol, 0.75 g) were dissolved in ethanol (50 mL). The above solution was refluxed at 80 °C for 8 h. After completion of reaction, further purified by silica gel column chromatography. ^{D}**7** was synthesized as the same procedures as ^{L}**7**.

Other imide derivatives were synthesized according to the previous report ref. S1–S6.

^{L}**1**, a total of 1.06 g (75% yield) of compound ^{L}**1** was obtained as a white crystal. ^{1}H NMR (400 MHz, DMSO-d_6) δ 8.12 – 7.94 (m, 2H), 7.83 – 7.71 (m, 1H), 4.91 (dd, J = 6.7, 5.4 Hz, 1H), 4.36 – 4.13 (m, 1H), 3.82 (ddd, J = 11.1, 9.3, 5.4 Hz, 1H), 3.53 (ddd, J = 11.1, 6.8, 5.4 Hz, 1H), 1.31 (d, J = 7.1 Hz, 3H). ^{13}C NMR (101 MHz, DMSO-d_6) δ 167.90, 167.31, 137.46, 134.11, 131.06, 128.28, 126.22, 125.20, 62.16, 49.81, 14.80. HRMS $[M+H]^+$, ($C_{11}H_{11}BrNO_3^+$), Cal: 283.9917, found: 283.9926.

^{D}**1**, a total of 0.99 g (70% yield) of compound ^{D}**1** was obtained as a white crystal.

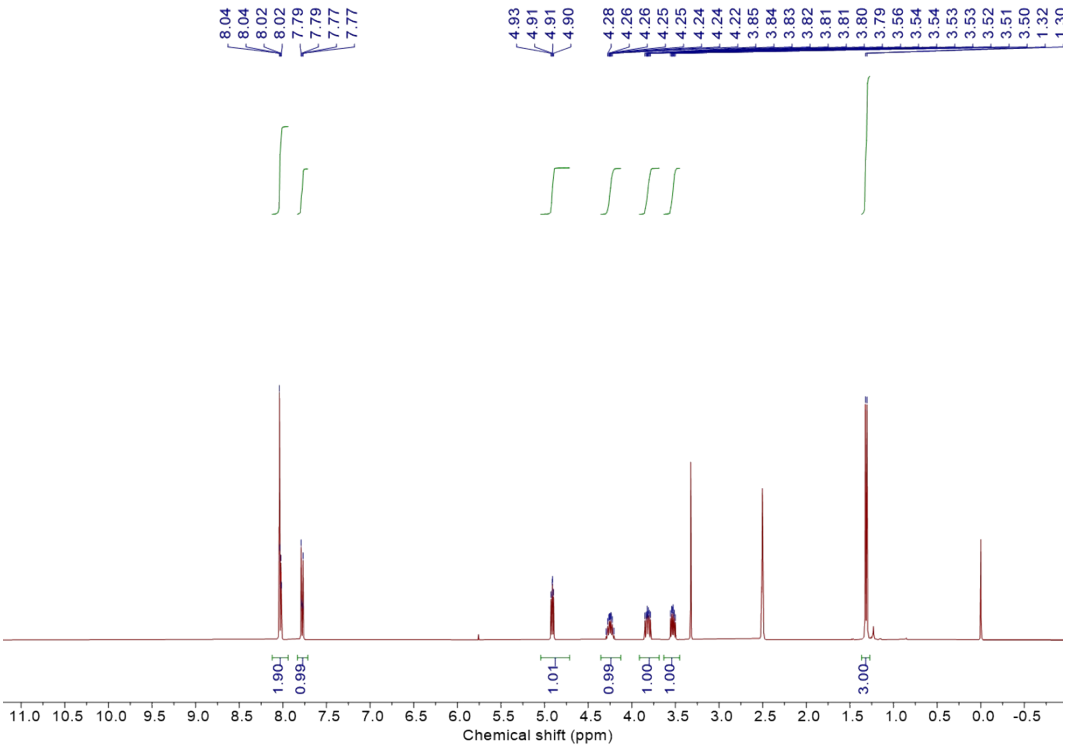

Figure S1. ^{1}H NMR spectrum of ^{L}**1** in DMSO-d$_6$.

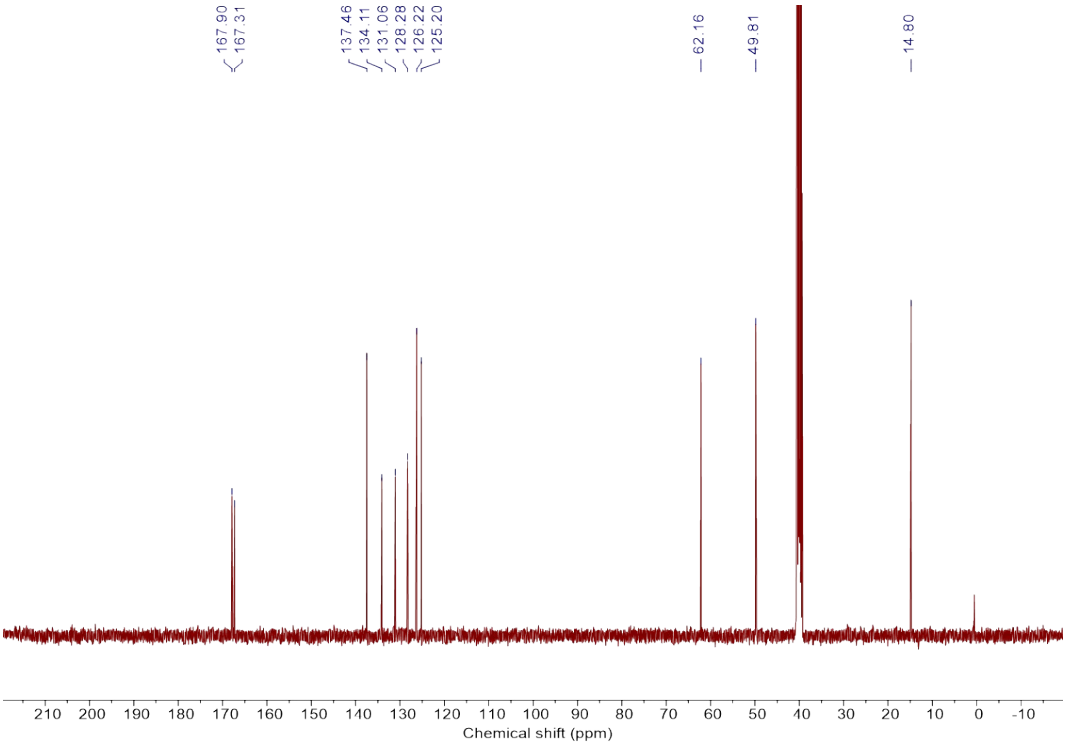

Figure S2. ^{13}C NMR spectrum of ^{L}**1** in DMSO-d$_6$.

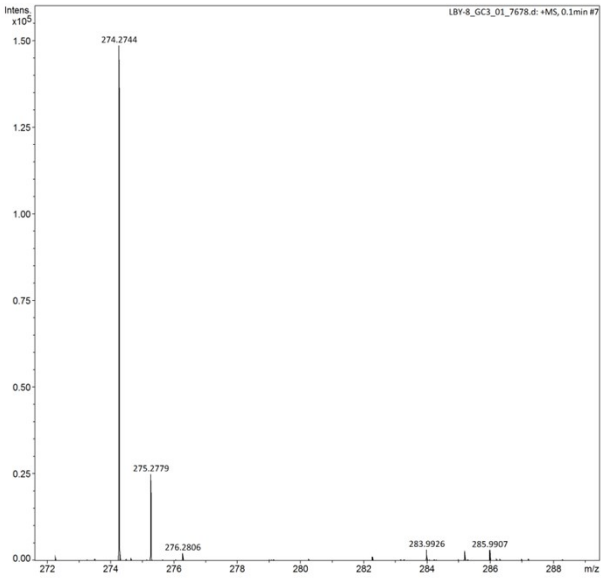

Figure S3. HRMS spectrum of ^{L}**1**.

^{L}**2**, a total of 1.17 g (65% yield) of compound ^{L}2 was obtained as a white crystal. ^{1}H NMR (400 MHz, DMSO-d_6) δ 7.99 (ddt, J = 4.7, 2.9, 1.6 Hz, 2H), 7.79 – 7.67 (m, 1H), 7.25 – 7.15 (m, 2H), 7.11 (dq, J = 8.6, 2.2 Hz, 3H), 5.00 (dd, J = 7.0, 5.3 Hz, 1H), 4.43 (tt, J = 10.2, 4.7 Hz, 1H), 3.95 (ddd, J = 11.2, 9.3, 5.3 Hz, 1H), 3.68 (ddd, J = 11.2, 7.0, 5.1 Hz, 1H), 3.08 (qd, J = 13.8, 8.0 Hz, 2H). ^{13}C NMR (101 MHz, DMSO-d_6) δ 167.83, 167.26, 138.52, 137.64, 133.59, 130.55, 129.08, 128.82, 128.50, 126.81, 126.31, 125.26, 61.06, 56.23, 34.32. HRMS $[M+H]^+$, ($C_{17}H_{15}BrNO_3$+), Cal: 360.0230, found: 360.0731.

^{D}**2**, a total of 1.22 g (65% yield) of compound ^{D}**1** was obtained as a white crystal.

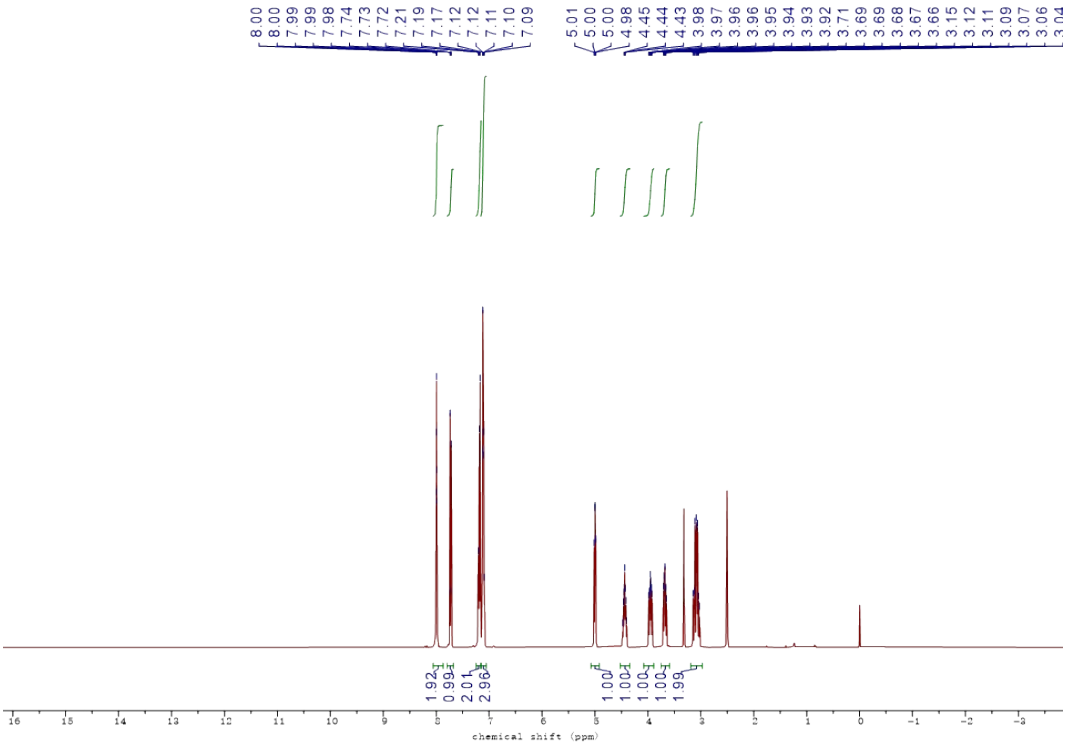

Figure S4. ^{1}H NMR spectrum of ^{L}**2** in DMSO-d$_6$.

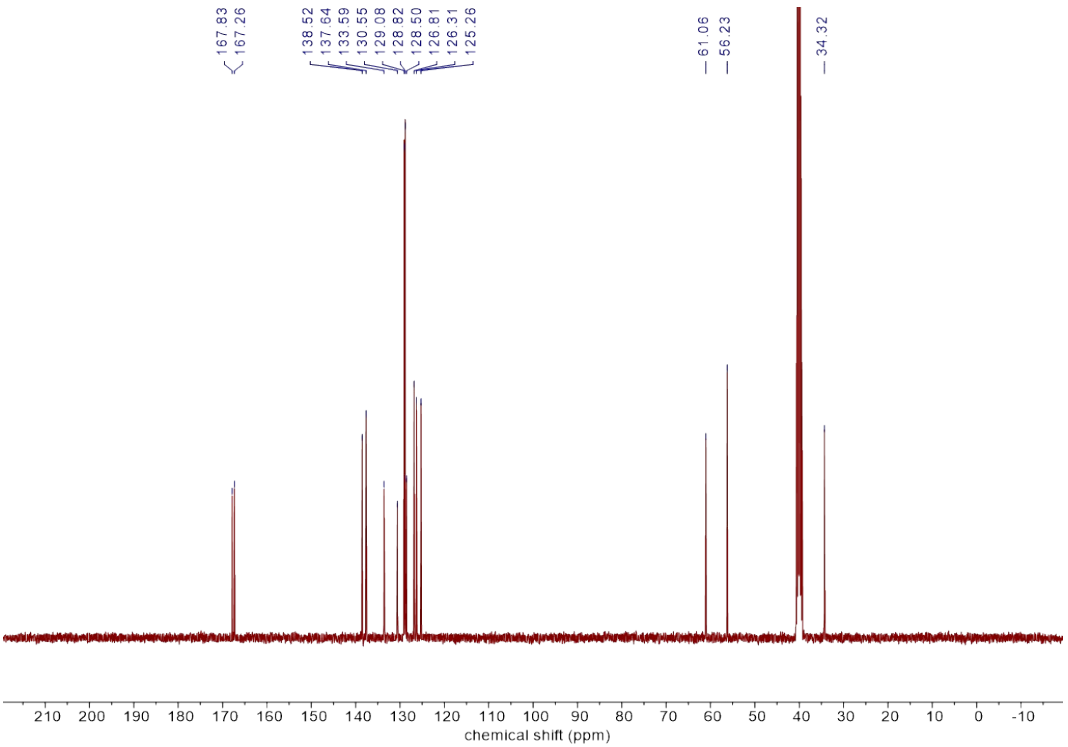

Figure S5. ^{13}C NMR spectrum of ^{L}**2** in DMSO-d$_6$.

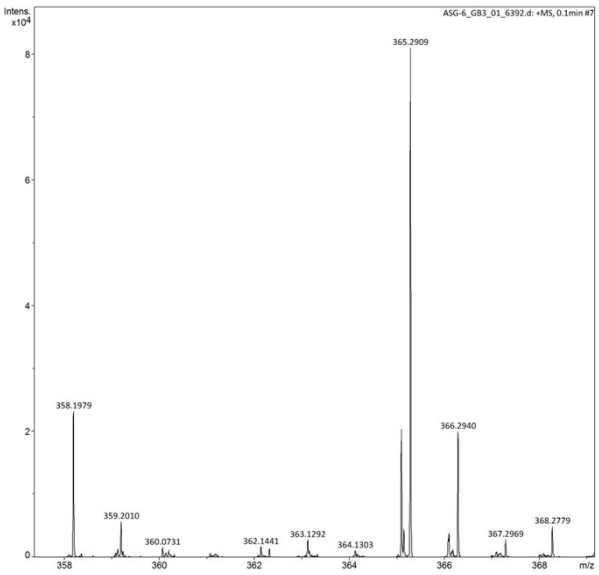

Figure S6. HRMS spectrum of ^{L}**2**.

^{L}**7**, a total of 1.12 g (55% yield) of compound ^{L}7 was obtained as an off-white powder. ^{1}H NMR (400 MHz, DMSO-d_6) δ 8.47 (d, J = 8.4 Hz, 2H), 8.17 (d, J = 7.6 Hz, 2H), 7.96 (d, J = 6.7 Hz, 1H), 7.23 – 7.09 (m, 4H), 7.06 (qd, J = 6.6, 5.7, 3.8 Hz, 1H), 5.45 (tt, J = 9.1, 5.9 Hz, 1H), 4.91 (t, J = 5.9 Hz, 1H), 4.17 (td, J = 10.8, 4.6 Hz, 1H), 3.79 (dt, J = 11.5, 5.9 Hz, 1H), 3.38 – 3.32 (m, 1H), 3.18 (dd, J = 13.7, 6.2 Hz, 1H). ^{13}C NMR (101 MHz, DMSO-d_6) δ 164.05, 139.17, 132.87, 131.86, 130.14, 129.35, 129.22, 128.78, 128.67, 126.60, 61.10, 57.45, 34.85. HRMS $[M+H]^+$, ($C_{21}H_{17}BrNO_3^+$), Cal: 410.0392, found: 410.1779.

^{D}**7** a total of 1.06 (52 yield) of compound ^{L}7 was obtained as an off-white powder.

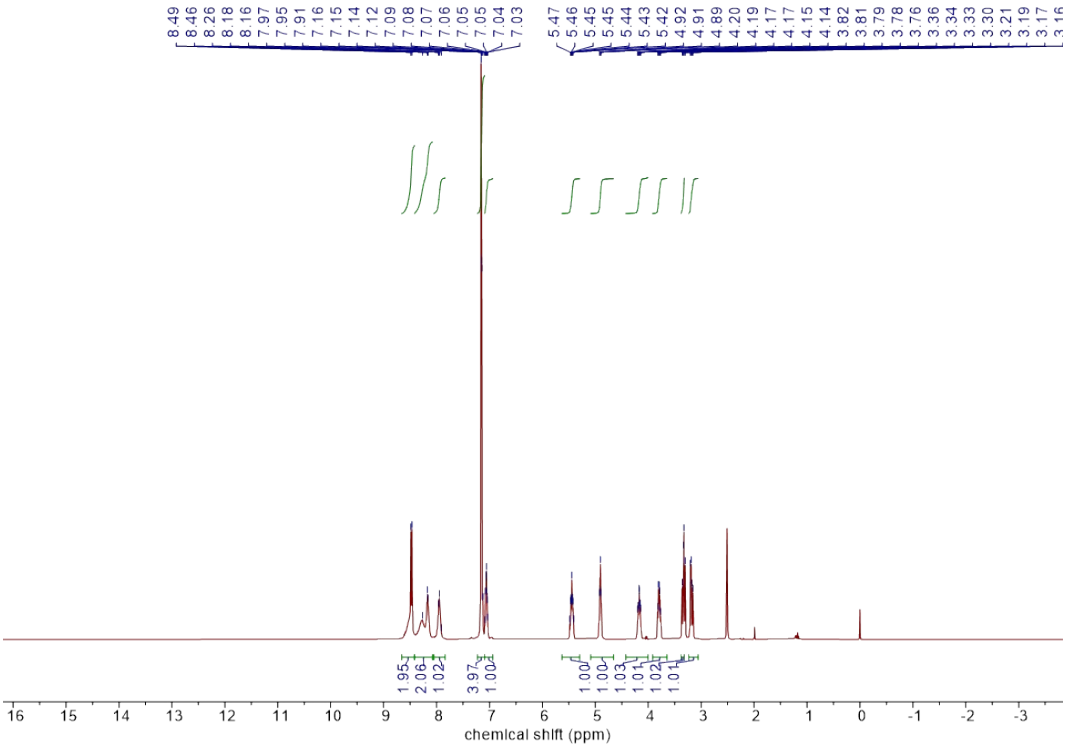

Figure S7. ^{1}H NMR spectrum of ^{L}**7** in DMSO-d$_6$.

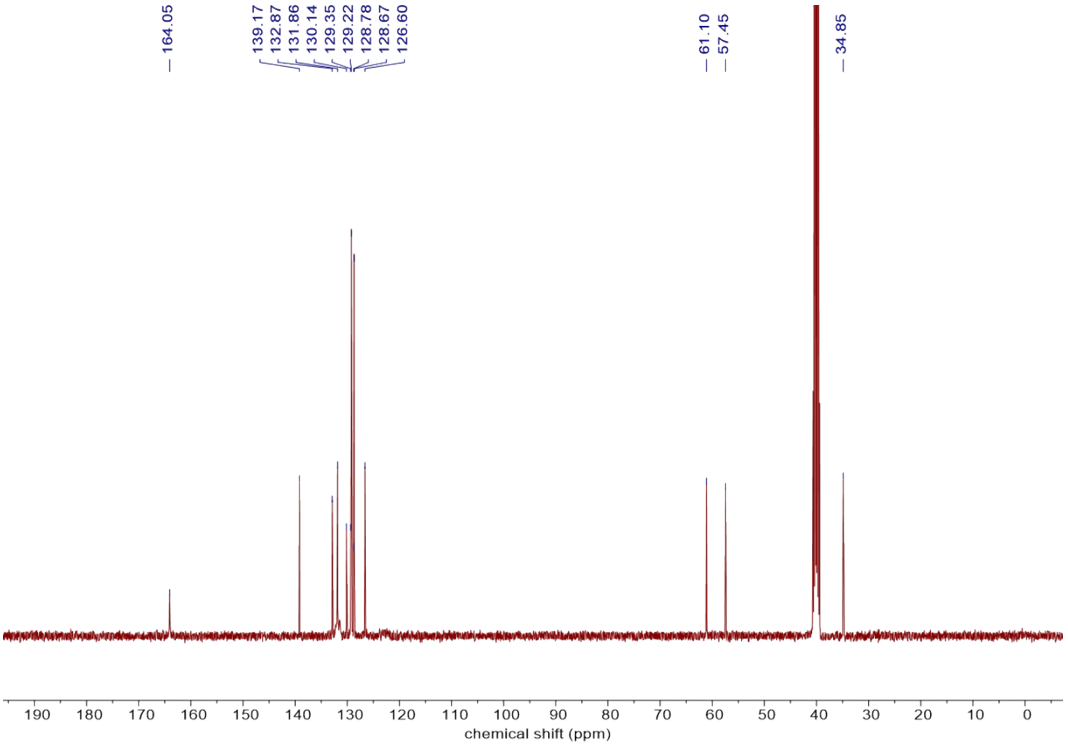

Figure S8. ^{13}C NMR spectrum of ^{L}**7** in DMSO-d$_6$.

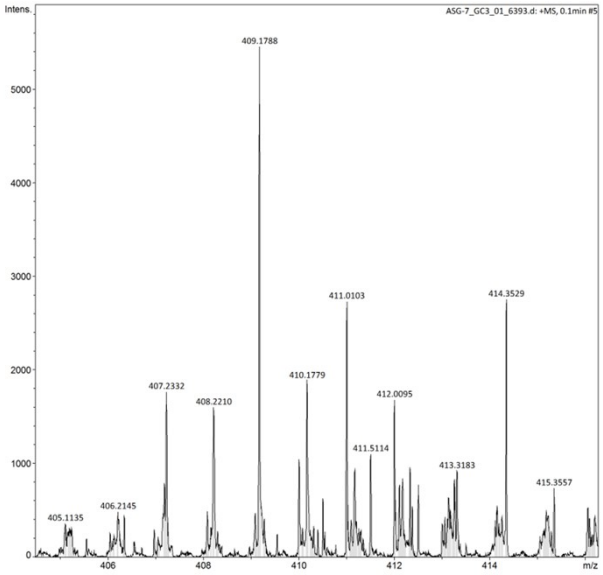

Figure S9. HRMS spectrum of ^{L}**7**.

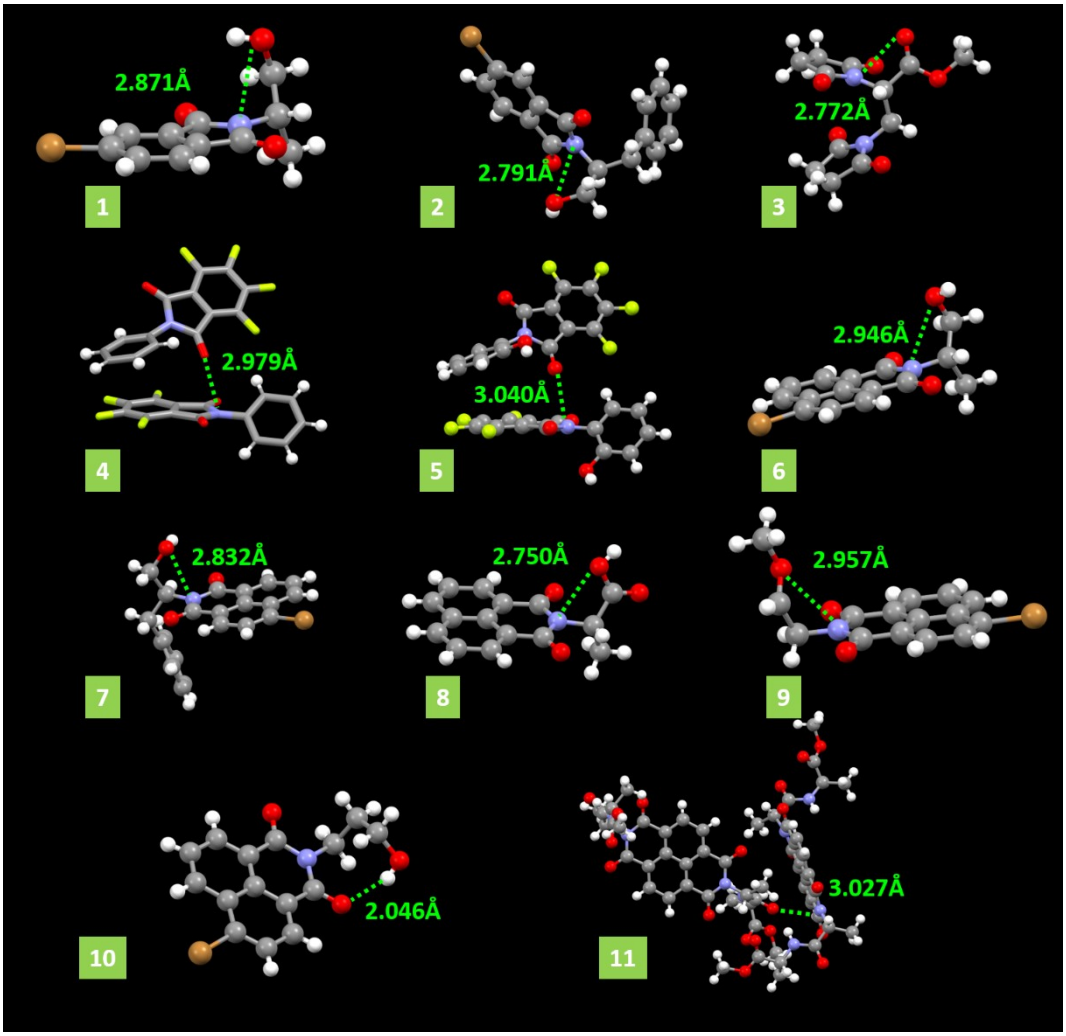

Figure S10. X-ray structures of PnB-containing imide derivatives.

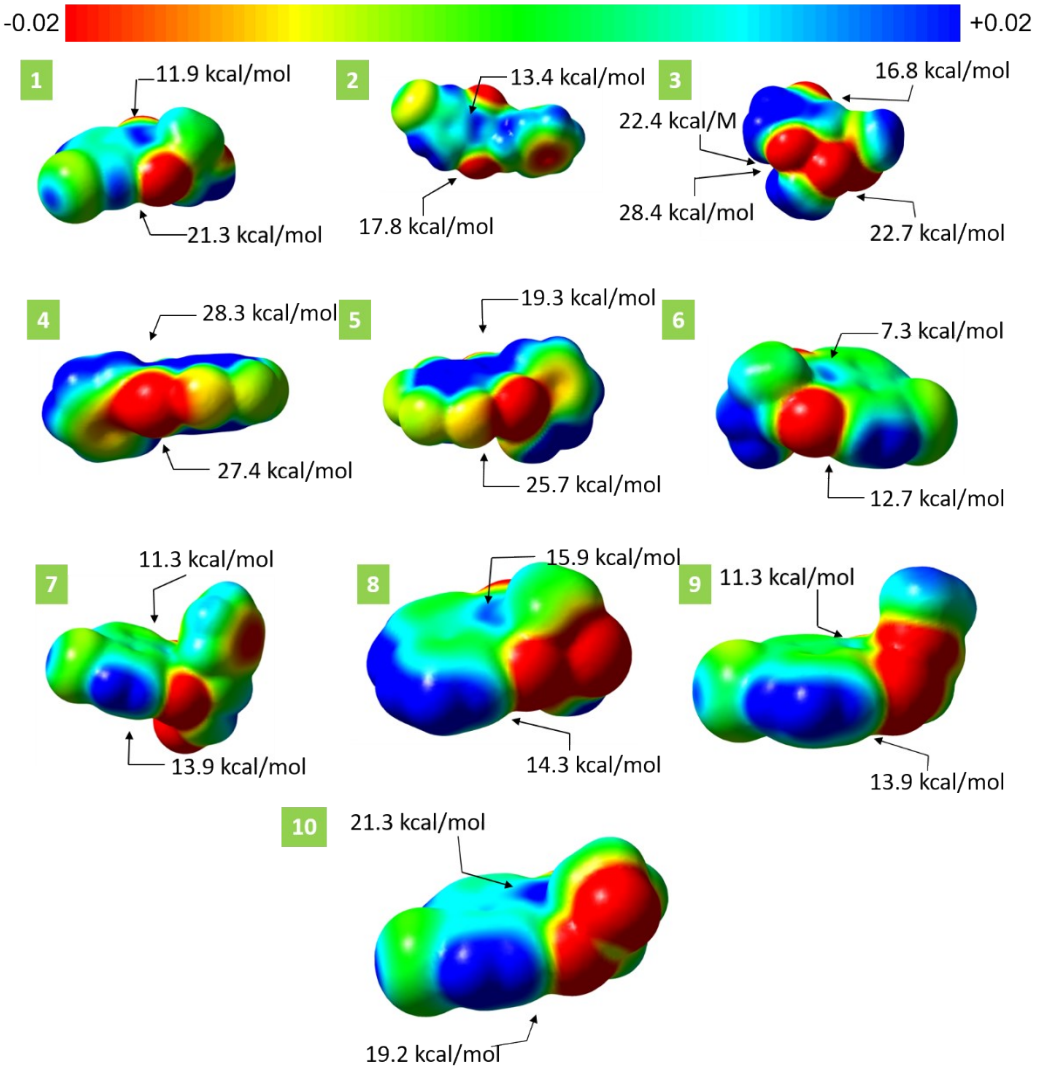

Figure S11. ESP maps of imide derivatives, as well as their extreme points on the both sides of imide N.

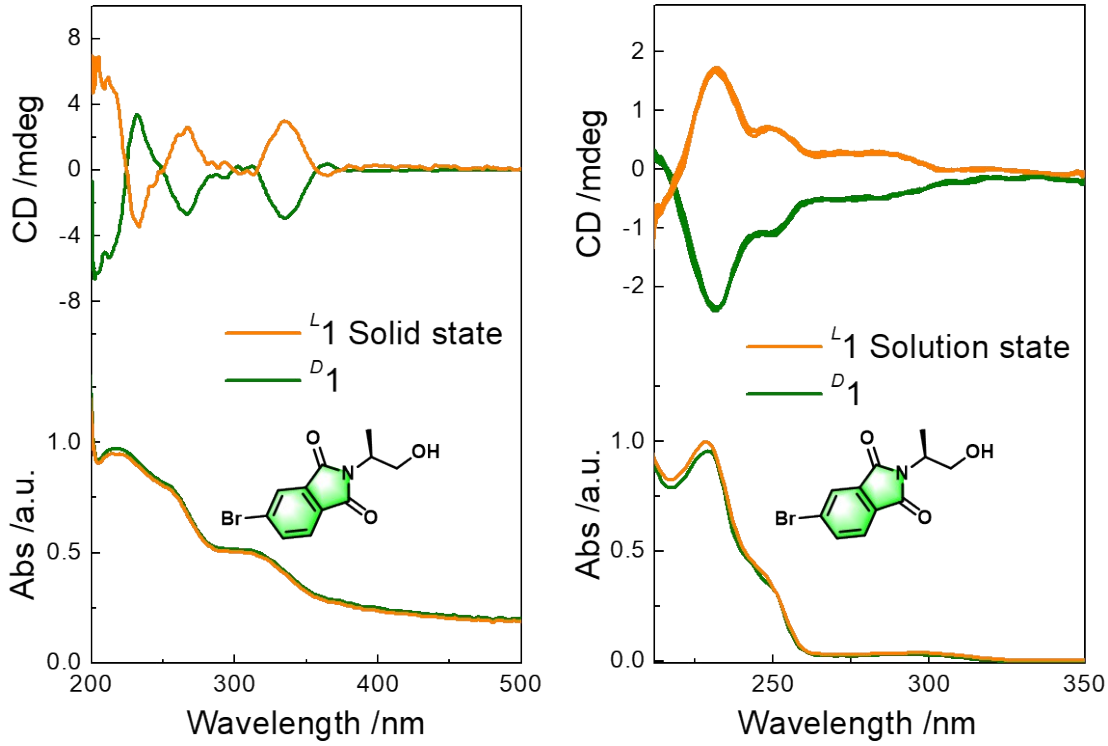

Figure S12. Solution state and solid state CD spectra of **1**.

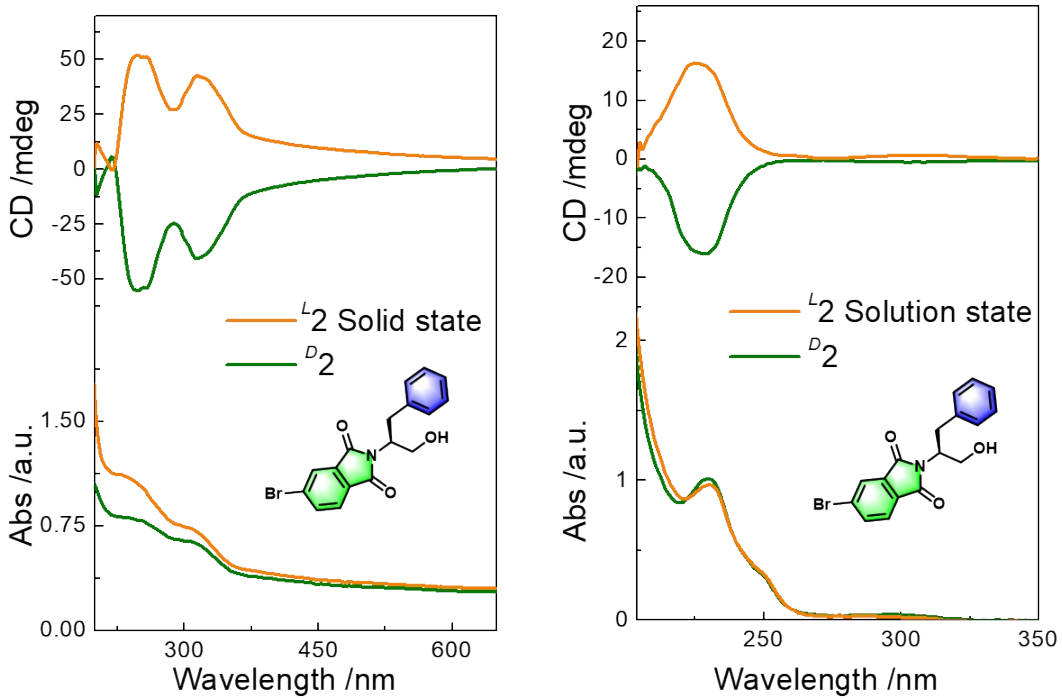

Figure S13. Solution state and solid state CD spectra of **2**.

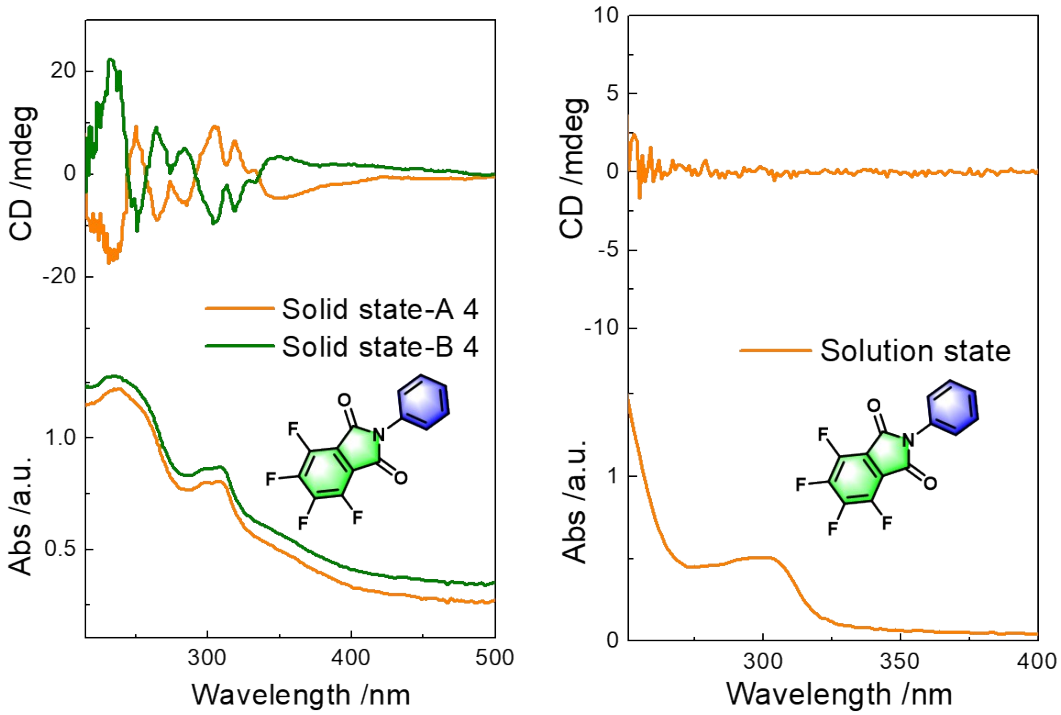

Figure S14. Solution state and solid state CD spectra of **4**.

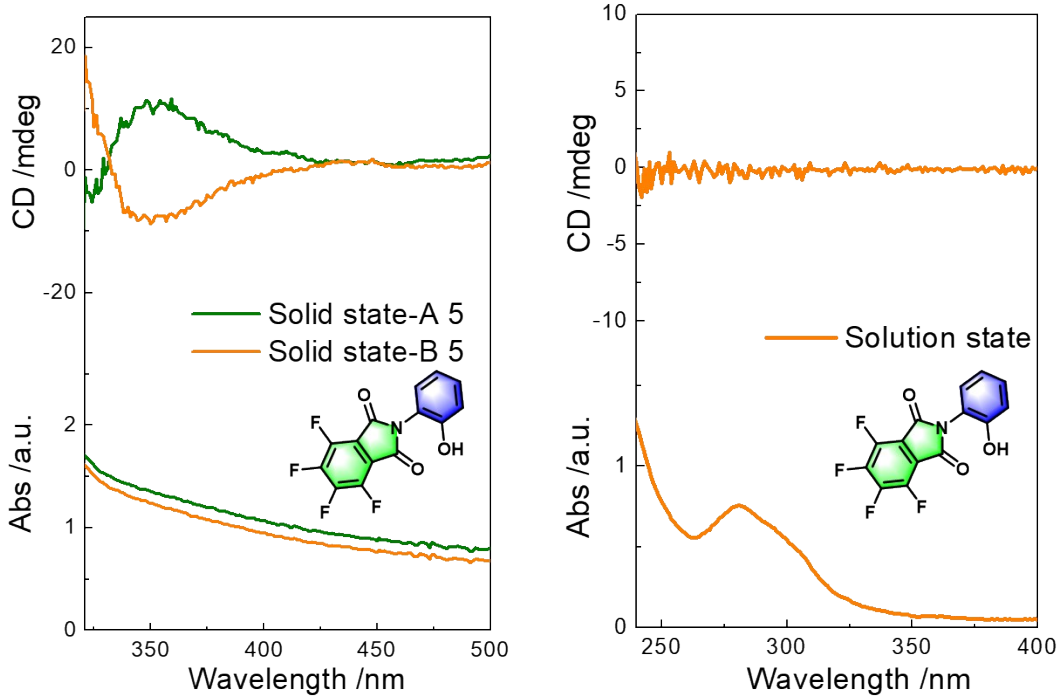

Figure S15. Solution state and solid state CD spectra of **5**.

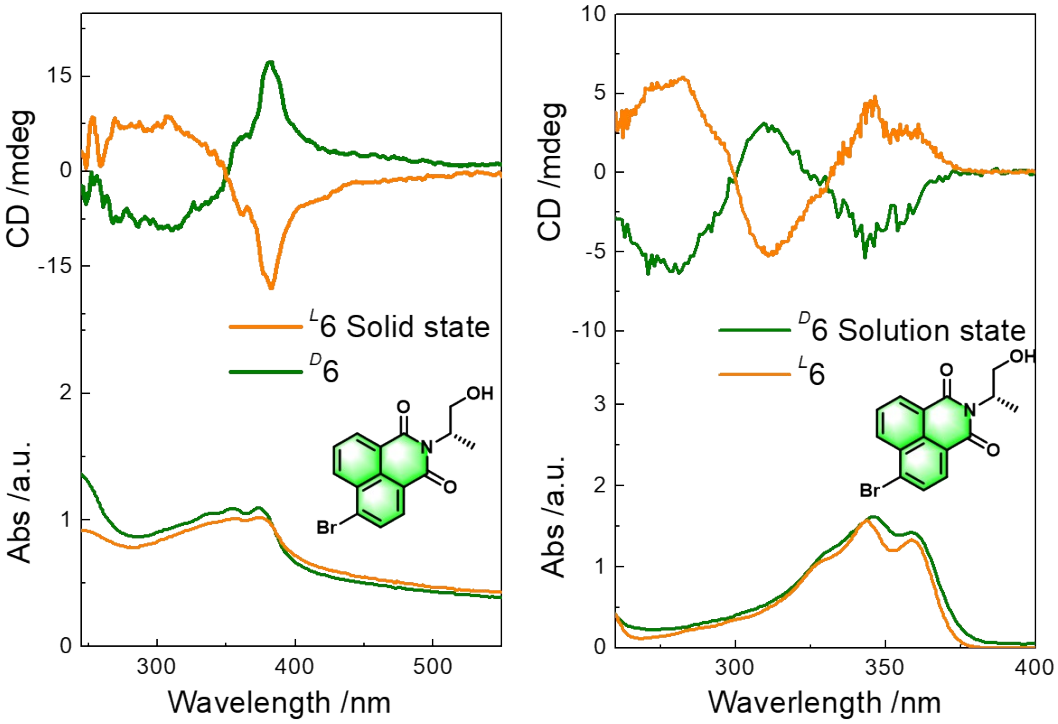

Figure S16. Solution state and solid state CD spectra of **6**.

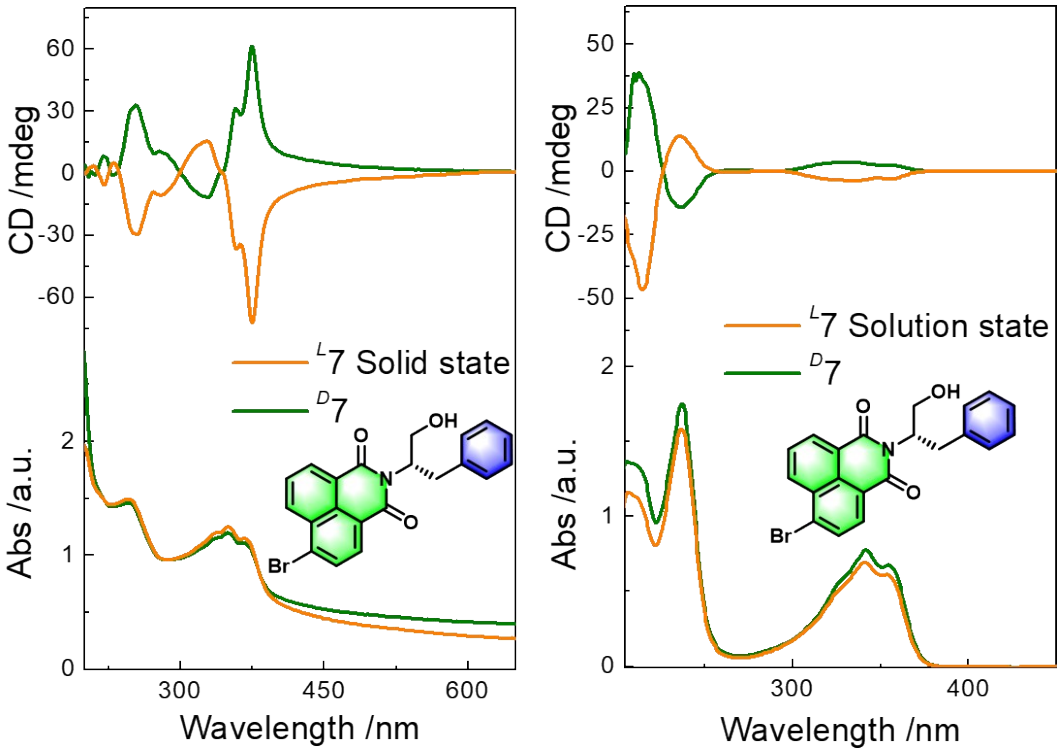

Figure S17. Solution state and solid state CD spectra of **7**.

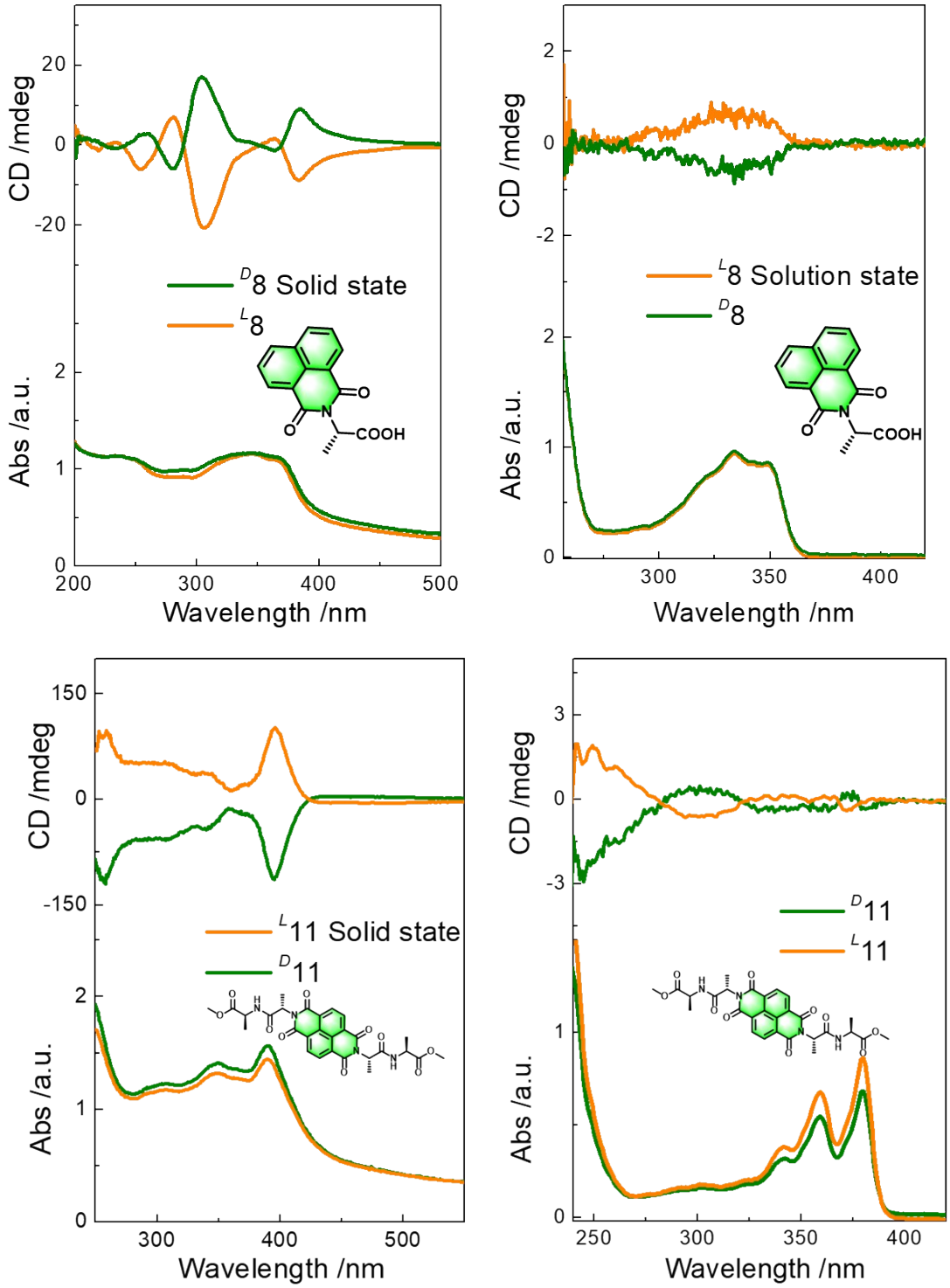

Figure S18. Solution state and solid state CD spectra of **8** and **11**, respectively.

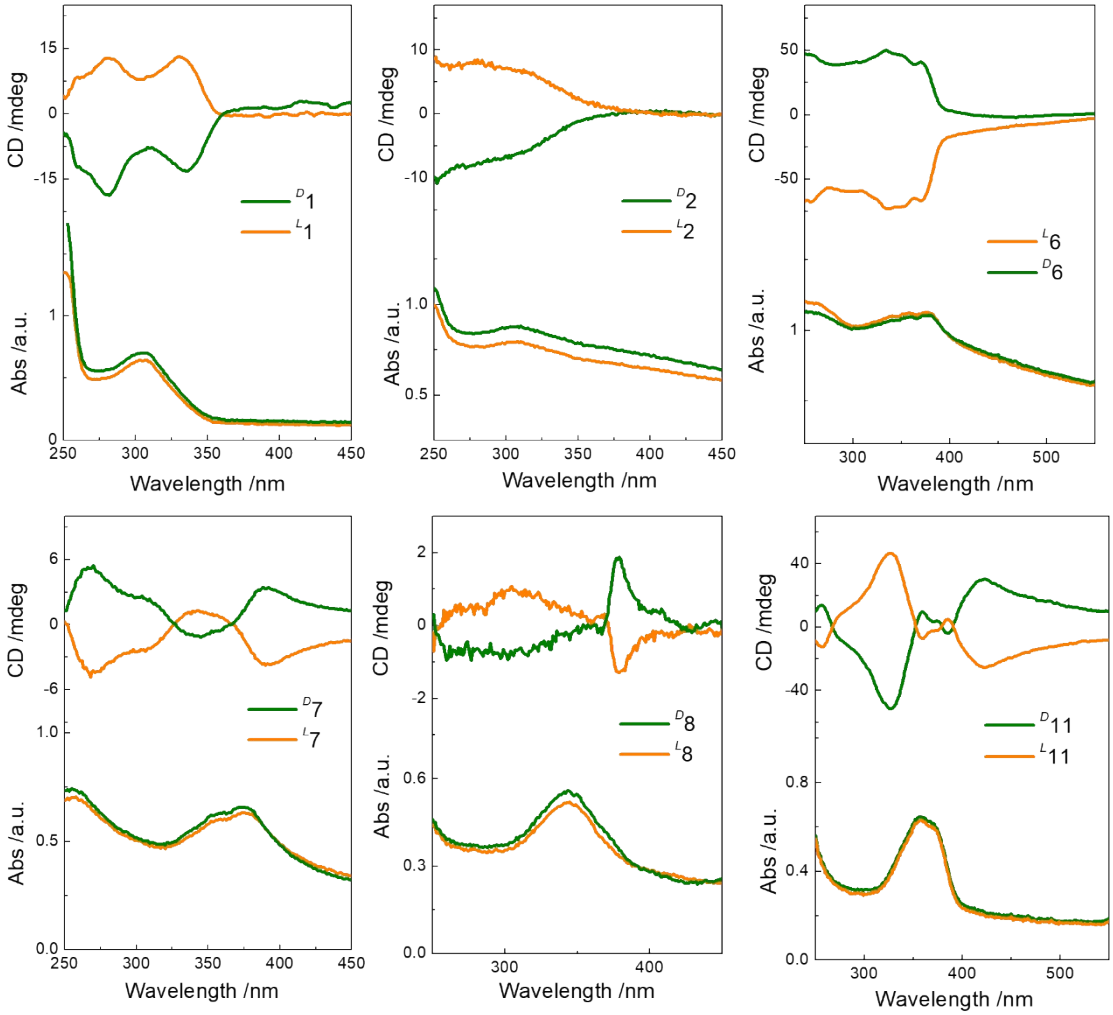

Figure S19. CD spectra of different self-assemblies in DMSO/H_2O (0.5:9.5 v/v, 5 mM).

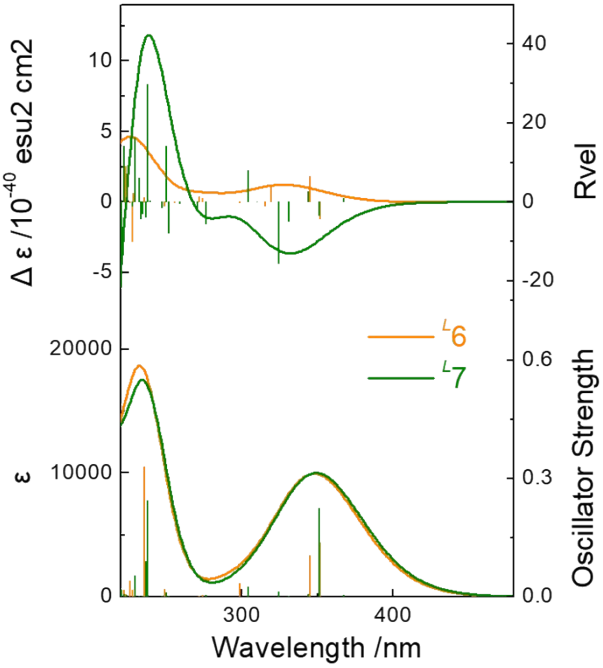

Figure S20.Calculated electronic CD spectra of ^{L}**6** and ^{L}**7** using the geometries found in crystal files.

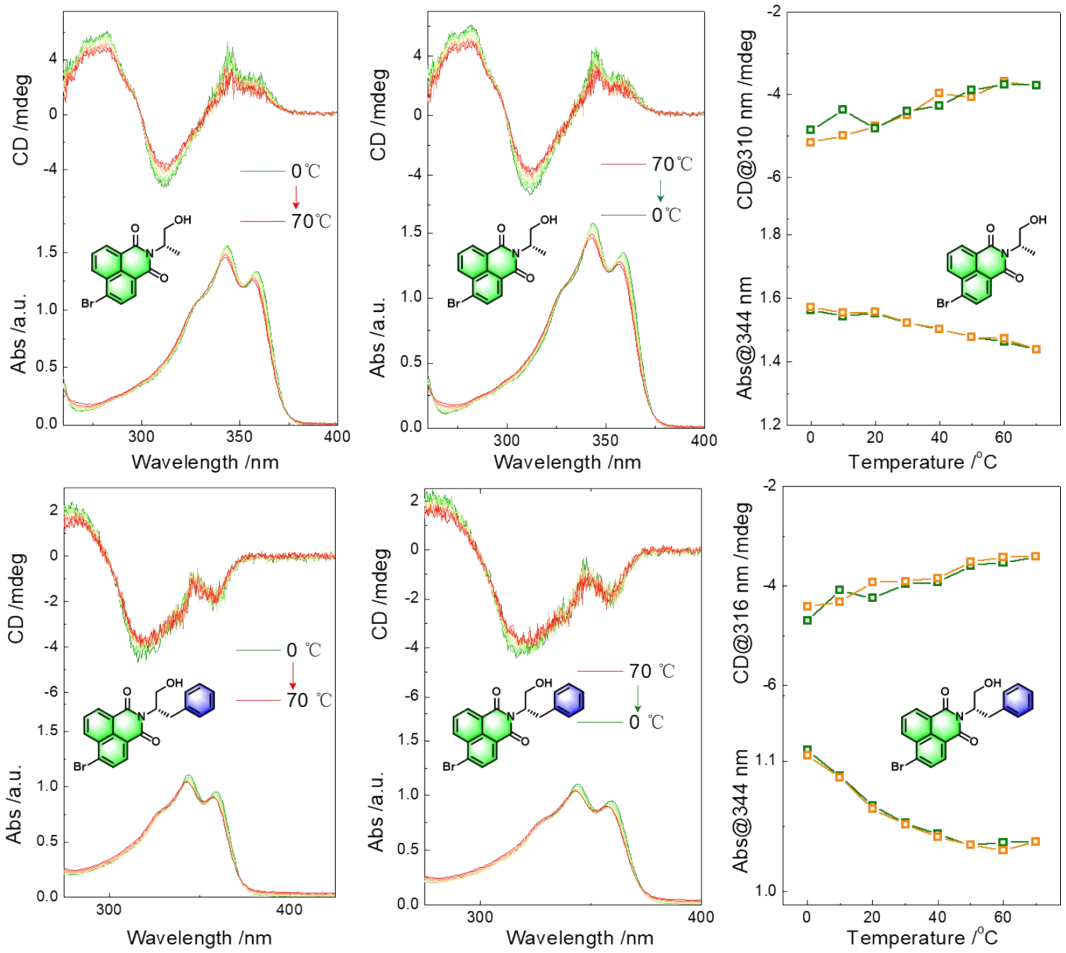

Figure S21. Temperature variable CD spectra of ^{L}6 and ^{L}7 (Dichloroethane, c = 0.4 mM).

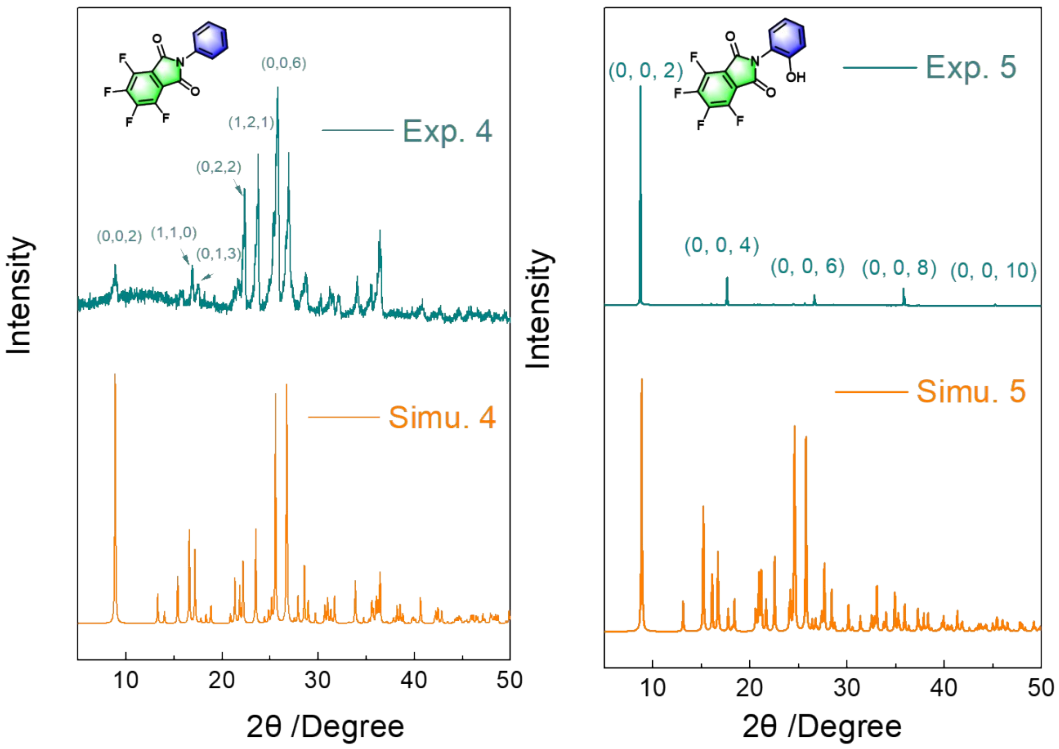

Figure S22. Simulated and experimental XRD pattern comparison of **4** and **5**.

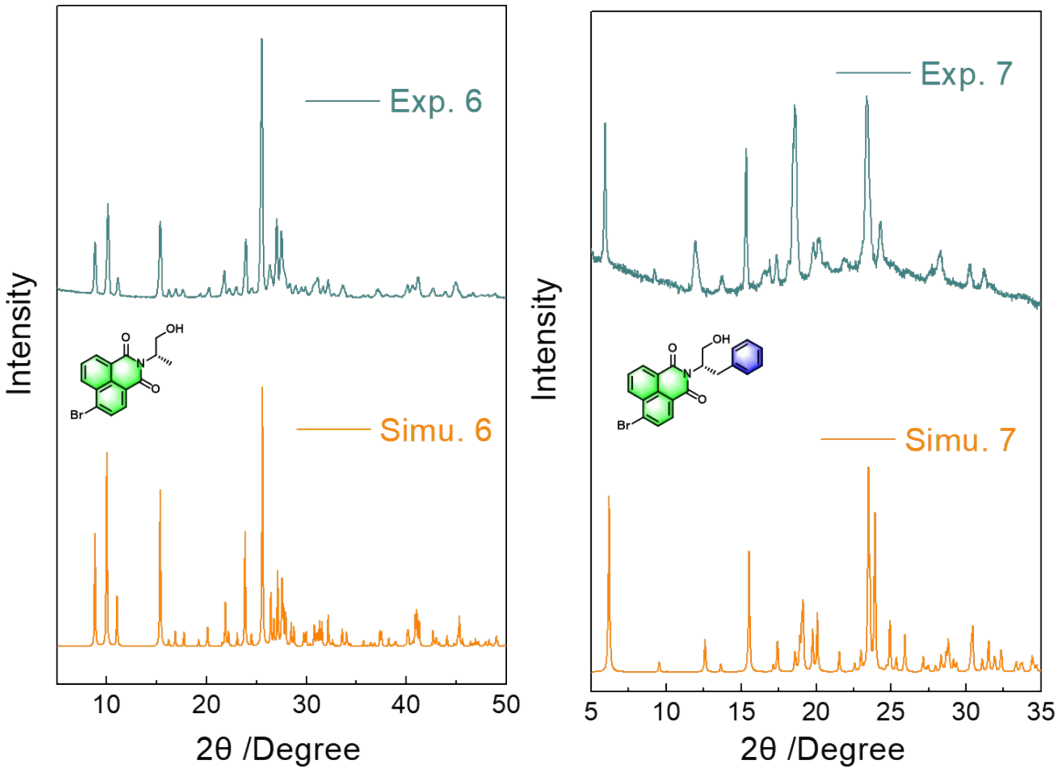

Figure S23. Simulated and experimental XRD pattern comparison of **6** and **7**.

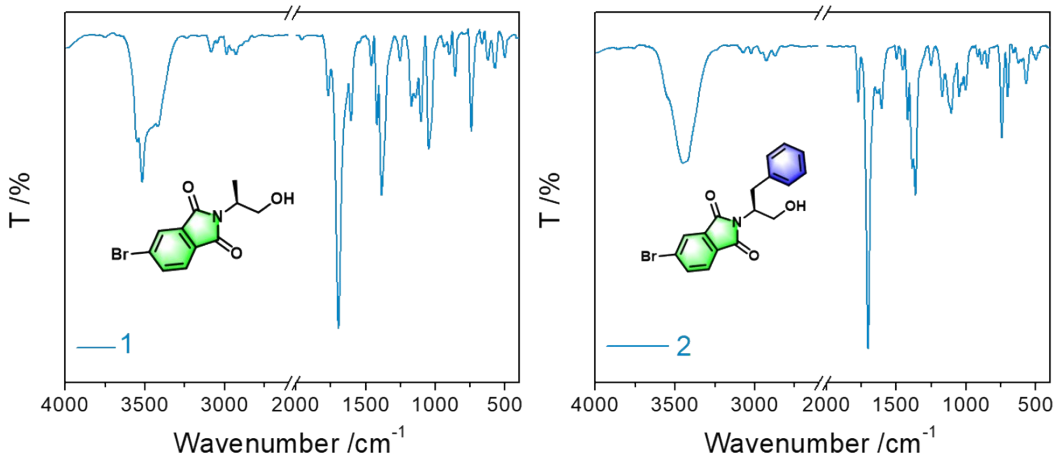

Figure S24. FT-IR spectra of **1** and **2**.

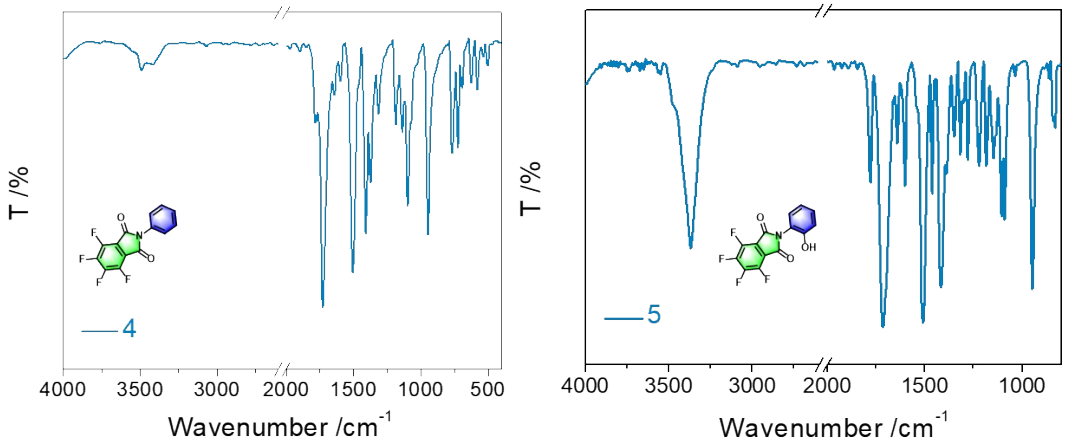

Figure S25. FT-IR spectra of **4** and **5**.

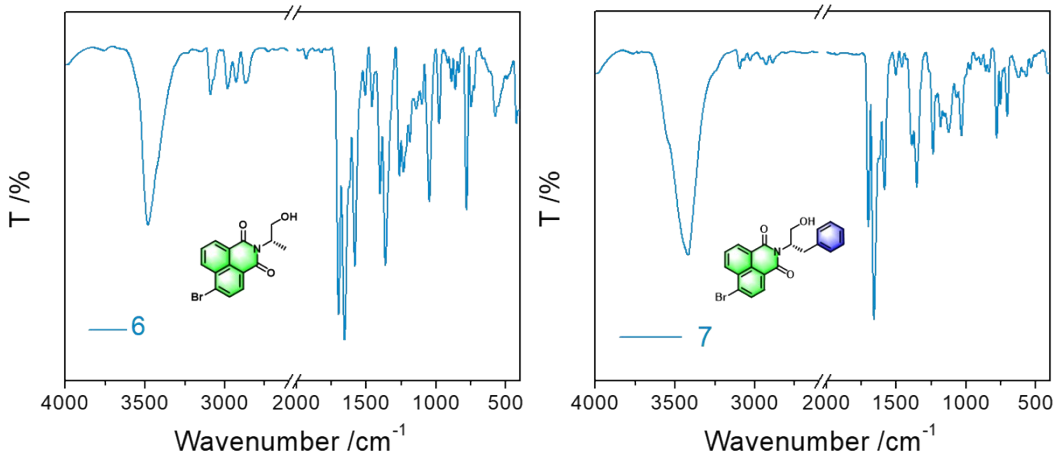

Figure S26. FT-IR spectra of **6** and **7**.

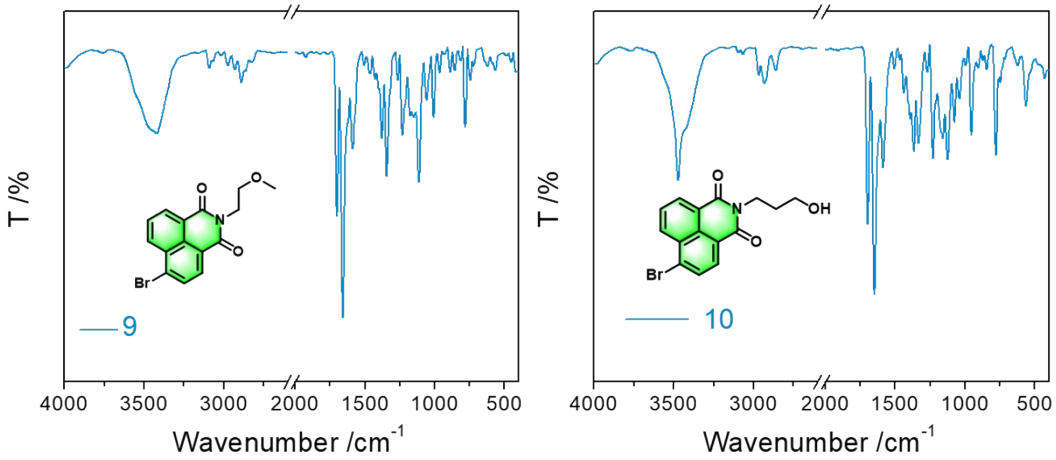

Figure S27. FT-IR spectra of **9** and **10**.

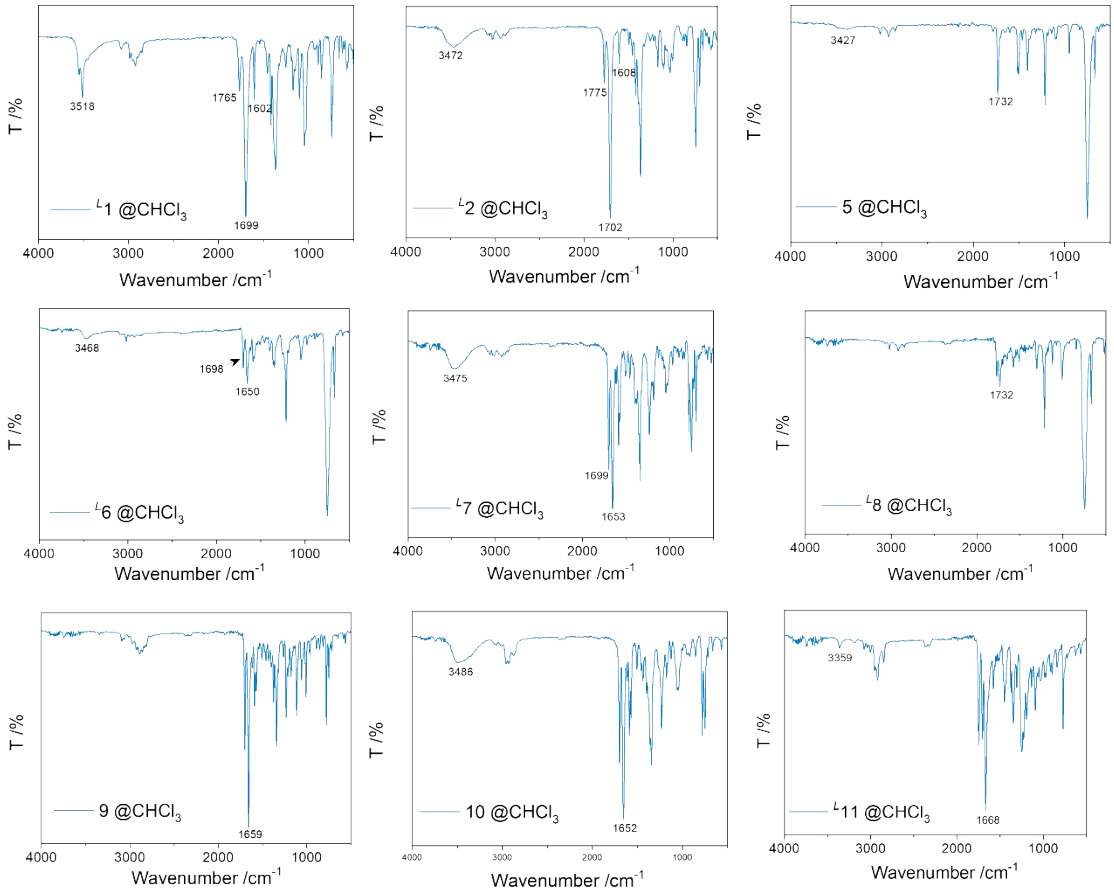

Figure S28. FT-IR spectra of different compounds in $CHCl_3$.

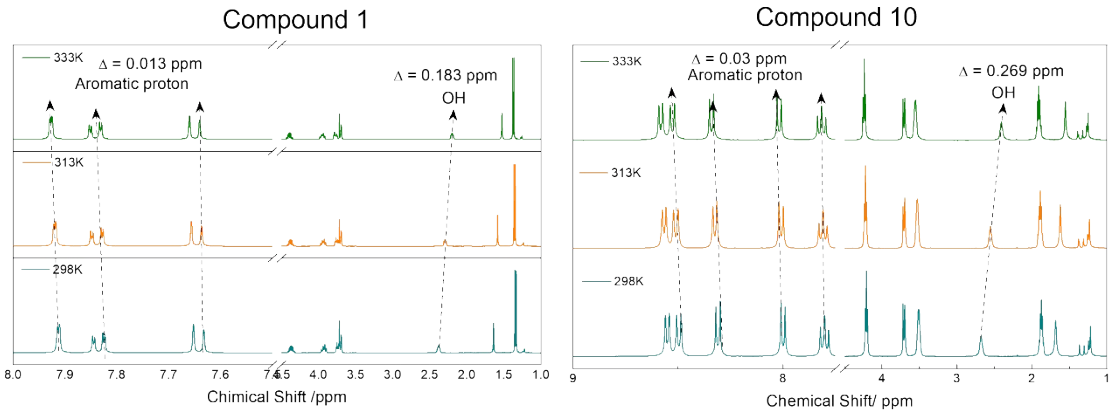

Figure S29. Temperature-variable 1H NMR spectra of compound 1 and 10 in dichloroethane-d_4.

Table S1 Crystal data of 1.

Deposition Number	2309600
Formula	C_{11} H_{10} Br N O_3
Temperature(K)	173.15
Wavelength	0.71073
Crystal system	monoclinic
Space group	P 2_1
a,b,c/Å	**a** 8.6432 **b** 5.5418 **c** 22.9285
V, Å^3	1084.73
Cell angles	**α** 90 **β** 99.00 **γ** 90
Z, Z'	Z: 2 Z': 1
R-factor (%)	3.9

Table S2 Crystal data of 2.

Deposition Number	2309601
Formula	C_{17} H_{14} Br N O_3

Temperature(K)	173.15
Wavelength	1.54184
Crystal system	orthorhombic
Space group	P $2_12_12_1$
a,b,c/Å	**a** 6.3065 **b** 13.7236 **c** 34.6883
V, Å³	3002.2
Cell angles	**α** 90 **β** 90 **γ** 90
Z, Z'	Z: 4 Z': 1
R-factor (%)	12.54

Table S3 Crystal data of 7.

Deposition Number	2309599
Formula	C_{21} H_{16} Br N O_3
Temperature(K)	173.15
Wavelength	1.54184
Crystal system	monoclinic
Space group	P 2_1
a,b,c/Å	**a** 9.5671 **b** 6.22015 **c** 14.7354
V, Å³	849.678
Cell angles	**α** 90 **β** 104.31 **γ** 90
Z, Z'	Z: 2 Z': 1
R-factor (%)	3.7

Table S4 Crystal data of 9.

Deposition Number	2309598
Formula	C_{15} H_{11} Br_1 N O_3
Temperature(K)	173.15
Wavelength	0.71073
Crystal system	triclinic
Space group	P -1
a,b,c/Å	**a** 7.4015 **b** 8.5478 **c** 11.0934
V, Å^3	647.623
Cell angles	**α** 96.710 **β** 92.275 **γ** 111.131
Z, Z'	Z: 2 Z': 1
R-factor (%)	4.88

Table S4 Crystal data of 10.

Deposition Number	2309602
Formula	C_{15} H_{11} Br_1 N O_3
Temperature(K)	173.15
Wavelength	0.71073
Crystal system	monoclinic
Space group	P 2_1/c
a,b,c/Å	**a** 7.3573 **b** 8.0361 **c** 21.7154
V, Å^3	1281.08
Cell angles	**α** 90 **β** 93.798 **γ** 90
Z, Z'	Z: 4 Z': 1
R-factor (%)	5.42

Table S5. Parameters of PnB of different compounds.

Compound	Bond type	Bond length/ Å	Bond angles/°	ESP/ kcal/M	NBO	Space group
1	O…N_{intra}	2.871	58.00	21.3	0	$P2_1$
2	O…N_{intra}	2.793	61.49	17.8	-	$P2_12_12_1$
3	O…N_{intra}	2.772	60.03	28.4	-	$Pca2_1$
4	O…N_{inter}	2.979	107.49	27.4	-	$P2_12_12_1$
5	O…N_{inter}	3.040	107.19	25.7	-	$P2_12_12_1$
6	O…N_{intra}	2.946	53.83	12.7	-	$P2_1$
7	O…N_{intra}	2.832	60.20	13.9	-	$P2_1$
8	O…N_{intra}	2.750	60.66	15.9	-	$P2_1$
9	O…N_{intra}	2.957	53.30	13.9	0	P-1
10	O…N_{intra}	3.632	54.02	21.3	0	$P2_1/C$
11	O…N_{inter}	3.027	118.16	-	-	$P2_12_12_1$
12	O…N_{intra}	2.816	58.35	-	-	$P2_1/n$
	S…N_{intra}	3.211	61.15			
	S…N_{intra}	3.211	60.31			
	O…N_{intra}	2.846	55.66			
13	O…N_{intra}	2.764	61.42	-		$P2_12_12_1$
	S…N_{intra}	3.168	62.22			
	S…N_{intra}	3.062	85.91			
	O…N_{intra}	2.649	82.49			

Table S6 Potential N…π interactions for each compound

Compound	d/ Å	Angles/ °	The n → π* Interaction	Deposition Nos
1	$d_{C...O}$ = 3.334	∠OC…O = 86.00	N (No)	CCDC: 2309600
	$d_{C...O}$ = 3.759	∠OC…O = 105.47	N	
2	$d_{C...O}$ = 3.194	∠OC…O = 89.09	N	CCDC: 2309601
	$d_{C...O}$ = 3.446	∠OC…O = 102.37	N	
3	$d_{C...O}$ = 3.142	∠OC…O = 76.95	N	CCDC: 2009253
	$d_{C...O}$ = 3.702	∠OC…O = 105.47	N	
4	$d_{C...O}$ = 2.864	∠OC…O = 104.41	Y (Yes)	CCDC: 654912
	$d_{C...O}$ = 3.218	∠OC…O = 117.14	Y	
5	$d_{C...O}$ = 2.945；	∠OC…O = 103.75	Y	CCDC: 667404
	$d_{C...O}$ = 3.251.	∠OC…O = 113.83	N	
6	$d_{C...O}$ = 3.416	∠OC…O = 82.50	N	CCDC: 2271094
	$d_{C...O}$ = 3.795	∠OC…O = 97.32	N	
7	$d_{C...O}$ = 3.351	∠OC…O = 90.66	N	CCDC: 2309599
	$d_{C...O}$ = 3.410	∠OC…O = 92.24	N	

8	$d_{C...O}$ = 3.076	∠OC…O = 73.79	N	CCDC: 844095
	$d_{C...O}$ = 3.719	∠OC…O = 100.75	N	
9	$d_{C...O}$ = 3.388	∠OC…O = 78.11	N	CCDC: 2309598
	$d_{C...O}$ = 3.837	∠OC…O = 96.01	N	
10	$d_{C...O}$ = 3.496	∠OC…O = 47.32	N	CCDC: 2309602
	$d_{C...O}$ = 4.867	∠OC…O = 107.76	N	
11	$d_{C...O}$ = 3.034	∠OC…O = 114.30	Y	CCDC: 1015723
	$d_{C...O}$ = 3.092	∠OC…O = 118.69	Y	
12	$d_{C...O}$ = 3.464	∠OC…O = 88.19	N	CCDC: 1970361
	$d_{C...O}$ = 3.663	∠OC…O = 97.94	N	
	$d_{C...S}$ = 3.630	∠OC…S = 85.03	N	
	$d_{C...S}$ = 3.991	∠OC…S = 100.99	N	
	$d_{C...S}$ = 3.627	∠OC…S = 84.58	N	
	$d_{C...S}$ = 4.080	∠OC…S = 103.97	N	
	$d_{C...O}$ = 3.159	∠OC…O = 78.35	N	
	$d_{C...O}$ = 3.752	∠OC…O = 104.28	N	
13	$d_{C...O}$ = 3.002	∠OC…O = 89.14	N	CCDC: 129316
	$d_{C...O}$ = 3.319	∠OC…O = 103.17	N	
	$d_{C...S}$ = 3.871	∠OC…S = 88.58	N	
	$d_{C...S}$ = 4.024	∠OC…S = 95.00	N	
	$d_{C...S}$ = 3.593	∠OC…S = 86.38	N	
	$d_{C...S}$ = 3.998	∠OC…S = 100.73	N	
	$d_{C...O}$ = 3.210	∠OC…O = 83.60	N	
	$d_{C...O}$ = 3.578	∠OC…O = 99.60	N	
Ala	$d_{C...O}$ = 3.143	∠OC…O = 82.89	N	CCDC: 112786
	$d_{C...O}$ = 3.628	∠OC…O = 105.82	N	
Val	$d_{C...O}$ = 3.059	∠OC…O = 88.73	N	CCDC: 320268
	$d_{C...O}$ = 3.376	∠OC…O = 103.69	N	
His	$d_{C...O}$ = 3.198	∠OC…O = 86.24	N	CCDC: 1021686
	$d_{C...O}$ = 3.272	∠OC…O = 91.39	N	
Phe	$d_{C...O}$ = 2.995	∠OC…O = 84.69	N	CCDC: 866278
	$d_{C...O}$ = 3.464	∠OC…O = 106.25	N	
	$d_{C...O}$ = 2.995	∠OC…O = 84.69	N	
	$d_{C...O}$ = 3.464	∠OC…O = 106.25	N	
Gln	$d_{C...O}$ = 3.105	∠OC…O = 79.58	N	CCDC: 1965092
	$d_{C...O}$ = 3.693	∠OC…O = 107.84	N	
Leu	$d_{C...O}$ = 3.007	∠OC…O = 83.29	N	CCDC: 866281
	$d_{C...O}$ = 3.472	∠OC…O = 105.65	N	
	$d_{C...O}$ = 3.028	∠OC…O = 87.95	N	
	$d_{C...O}$ = 3.335	∠OC…O = 103.31	N	
Hydrolase	$d_{C...O}$ = 2.945	∠OC…O = 105.84	Y	PDB code：
	$d_{C...O}$ = 3.027	∠OC…O = 106.70	Y	1EMJ

Cartesian coordinates of the optimized structures

Computational details: All the geometries were optimized with Gaussian 16 program at the B3LYP-D3/def2SVP level. [S7]

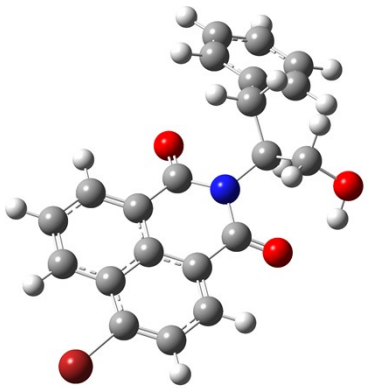

Transition state structure of ^{L}7, E = -3665.018953 Hartree, Imaginary frequency = 1

Br	-5.78878100	-0.20623000	0.14750200
O	1.76792700	-1.55611500	-0.00328000
N	1.10629300	0.63369000	-0.20132800
O	0.42077000	2.65057100	0.63994000
C	-0.54740200	-1.19912400	-0.17242000
C	2.49318900	1.17955600	-0.43641300
H	2.92691700	1.38104200	0.54266300
O	2.69617300	3.66012800	-0.35903600
H	1.96916100	3.69513800	0.27890900
C	2.42585100	2.54909100	-1.17996500
H	3.20247400	2.56350300	-1.94061300
H	1.46519800	2.64648600	-1.69888100
C	-2.28263400	1.98998500	0.47005700
H	-2.02656500	3.02131500	0.66710900
C	4.52443900	-0.41491800	-0.37201500
C	-1.27559000	1.07850300	0.24764200
C	-3.94560300	0.27475600	0.18449300
C	-0.82939200	-2.53132500	-0.37360200

H	-0.01048900	-3.22764900	-0.48684400
C	-1.59158300	-0.27052000	-0.00067800
C	6.63568900	-1.52154800	1.10307800
H	7.44866500	-1.95007100	1.67496200
C	5.80068800	-2.33859000	0.35095700
H	5.95875200	-3.40965200	0.33745200
C	6.41861800	-0.14873600	1.11479100
H	7.06554900	0.49912900	1.69259900
C	-3.62544700	1.58770300	0.43197200
H	-4.40947700	2.31200600	0.59768500
C	-2.16284500	-2.96646900	-0.42894400
H	-2.37449200	-4.01344900	-0.59910400
C	-3.19946900	-2.08065500	-0.26192300
H	-4.22208500	-2.42679100	-0.29666200
C	-2.94714600	-0.70970600	-0.03299400
C	5.37476700	0.39785300	0.37945400
H	5.22435000	1.47136700	0.38906200
C	3.42801500	0.20460700	-1.20570700
H	2.87016900	-0.56846000	-1.72301500
H	3.91598600	0.79010600	-1.98615700
C	4.75384400	-1.78795400	-0.37811900
H	4.09250800	-2.43189600	-0.94164300
C	0.13280800	1.52807200	0.25871500
C	0.86715100	-0.75501300	-0.11201000

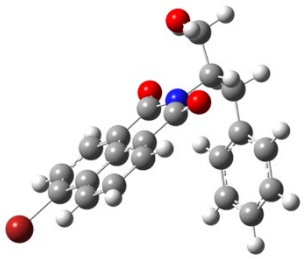

Optimized structure of $^{L}7$, E = -3665.044303 Hartree, Imaginary frequency = 0

Br	0	-4.99362500	-0.46766900	-0.31929900
O	0	2.02063900	1.91720200	1.79331200
N	-1	1.80816500	0.94328300	-0.25566500
O	0	1.50791400	0.26906900	-2.40676300
C	0	-0.14348500	1.17357200	1.21552500
C	-1	3.27859900	1.02079500	-0.43241600
H	0	3.64066400	1.20579300	0.57611300
O	-1	3.02712400	3.43353800	-0.83335300
H	0	3.13061100	3.49476100	0.12452000
C	0	3.65087000	2.23690400	-1.28399300
H	0	4.74413400	2.33181300	-1.27770000
H	0	3.32625300	2.09406200	-2.31274600
C	0	-1.21942300	-0.24637500	-2.02560500
H	0	-0.78041300	-0.49202500	-2.98235100
C	0	3.38346800	-1.48316600	-0.15538300
C	0	-0.41687400	0.28318400	-1.04171200
C	0	-3.13153800	-0.14578700	-0.57381600
C	0	-0.67295000	1.51810700	2.43867400
H	0	-0.01877100	1.94441300	3.18600400
C	0	-0.96609000	0.61725700	0.21280300
C	0	2.31314000	-3.63027000	1.29242300
H	0	1.89929000	-4.45895700	1.85223300
C	0	2.02784200	-3.48623600	-0.05913500
H	0	1.38889200	-4.20356200	-0.55841900
C	0	3.13746800	-2.70323600	1.92142500
H	0	3.36838300	-2.80852500	2.97379900
C	0	-2.58383100	-0.46606300	-1.79174200
H	0	-3.20459300	-0.88615500	-2.56953700

C	0	-2.03558300	1.31165100	2.70046300
H	0	-2.44056000	1.58254400	3.66613300
C	0	-2.85849900	0.77027900	1.74361300
H	0	-3.90691400	0.61553600	1.95235100
C	0	-2.35330500	0.41006300	0.47439200
C	0	3.66673400	-1.64066700	1.20196000
H	0	4.30304500	-0.92084100	1.70328000
C	0	3.90755600	-0.29312800	-0.91822400
H	0	3.73861500	-0.42653100	-1.98296100
H	0	4.98529800	-0.19518600	-0.76240500
C	0	2.55895600	-2.41949400	-0.77574700
H	0	2.32320400	-2.30132700	-1.82547700
C	-1	1.02101900	0.49102300	-1.31411300
C	0	1.29878800	1.38677600	0.96672900

References:

S1. Schwarzer, A.; Weber, E. *Cryst. Growth Des.* **2008**, 8, 2862 -2874.

S2. Wang, Z.; Hao, A.; Xing, P. *Chem. Mater.* **2023**, 10.1021/acs.chemmater.3c02390.

S3. Chand, T.; Khamari, L.; Chopra, D.; Mukherjee, S.; Kapur, M. *Chem.-Eur. J.* **2022**, 28, e202200723.

S4. Rudebeck, E.; Cox, R.; Bell, T.; Acharya, M.; Feng, Z.; Gueven, N.; Ashton, T. and Pfeffer, F. *Chem. Commun.*, **2020**, 56 , 6866 -6869.

S5. Pandeeswar, M.; Khare, H.; Ramakumar, S.; Govindaraju, T. *Chem. Commun.*, **2015**, 51 , 8315 -8318.

S6. Biagini, S.; Bush, S.; Gibson, V.; Mazzariol, L.; North. M.; Teasdale, W.; Williams, C.; Zagotto, G.; Zamuner, D. *Tetrahedron.* **1995**, 51, 7247 -7262.

S7. Frisch, M. J.; Trucks, G. W.; Schlegel, H. B.; Scuseria, G. E.; Robb, M. A.;Cheeseman, J. R.; Scalmani, G.; Barone, V.; Petersson, G. A.; Nakatsuji, H.; Li, X.;Caricato, M.; Marenich, A. V.; Bloino, J.; Janesko, B. G.; Gomperts, R.; Mennucci, B.;Hratchian, H. P.; Ortiz, J. V.; Izmaylov, A. F. et al., Gaussian 16, Revision A.03;

Gaussian, Inc.: Wallingford, CT, 2016.